Reaction Chemistry & Engineering

ROYAL SOCIETY OF CHEMISTRY

PAPER

View Article Online
View Journal

Open Access Article. Published on 10 December 2025. Downloaded on 2/1/2026 6:07:50 PM.
This article is licensed under a Creative Commons Attribution 3.0 Unported Licence.

Check for updates

Cite this: DOI: 10.1039/d5re00337g

# Determination of reaction kinetics in three phase $CO_2$ methanation

Mathias Monning, *[a] Asad Asadli,[b] Siegfried Bajohr,[a] Moritz Wolf [ab] and Thomas Kolb [a]

Received 4th August 2025,
Accepted 25th November 2025

DOI: 10.1039/d5re00337g

rsc.li/reaction-engineering

In three phase $CO_2$ methanation, the hydrogenation of the liquid phase dibenzyl toluene (DBT) occurs as a side reaction in the liquid phase. Additionally, DBT decomposition leads to catalyst deactivation by carbon deposition on the catalytic surface. By analyzing the influence of catalyst deactivation on the reaction rates of $CO_2$ methanation and DBT hydrogenation, partial wetting of the catalyst particles is observed. The catalyst surface is not entirely covered by the liquid phase, instead small gas-filled pores remain, within which $CO_2$ methanation occurs in the gas phase. Reaction kinetics under steady state conditions at high reactor temperature is determined for $CO_2$ methanation.

## 1 Introduction

In future energy systems, the supply of electrical energy is expected to become more volatile due to fluctuating wind and solar power. To match energy supply and demand, processes that offer dynamic operability are needed. One such process is three phase $CO_2$ methanation in a slurry bubble column reactor: catalyst particles are suspended in the liquid phase dibenzyl toluene (DBT) and fluidized by the feed gas flow entering the reactor at the bottom. Due to the high heat capacity and high degree of mixing in the reactor, near isothermal and load-flexible operation is achievable.[1]

For reactor design and scale-up, reaction kinetics of three phase $CO_2$ methanation is essential. In the literature, different approaches to determine reaction kinetics in three phase systems are discussed: reaction kinetics can be derived using the gas-phase partial pressures of the educt and product gases or from their concentrations in the liquid phase. Typically, catalyst particles are assumed to be fully wetted by the liquid phase, and thus liquid phase concentrations are used to determine reaction kinetics.

In this work, a theory of partial wetting of catalyst particles by the liquid phase is introduced and validated: the catalyst pores are not completely filled with liquid, instead only a portion of the pore surface is covered. To validate this theory, the impact of catalyst deactivation due to DBT decomposition on the reaction rates of $CO_2$ methanation and DBT hydrogenation is evaluated. Furthermore, reaction kinetics under steady-state conditions for $CO_2$ methanation with catalyst deactivation is determined.

## 2 Theory

### 2.1 Catalytic $CO_2$ methanation

Catalytic $CO_2$ methanation was first described by Sabatier,[2] and its application in the Power-to-Gas process has been extensively discussed in the literature.[3,4] $CO_2$ and $H_2$ are converted to $CH_4$ and $H_2O$ according to eqn (1):

$$CO_2 + 4{\cdot}H_2 \rightleftharpoons CH_4 + 2{\cdot}H_2O \quad \Delta H_R = -165\ \text{kJ mol}^{-1} \tag{1}$$

Nickel is often used as an active component of catalysts, as it exhibits high activity for $CO_2$ methanation and high selectivity toward $CH_4$.[5,6] Typically, a reactor temperature above $T_R > 200$ °C is chosen to obtain high reaction rates. However, the maximum temperature is limited by thermal catalyst deactivation and the constraints of chemical equilibrium on achievable conversion. Moderate reactor pressures, up to $p_{R,abs} = 20$ bar, are commonly applied.

Various reactor concepts are employed for catalytic $CO_2$ methanation, including fixed-bed, fluidized-bed or micro-structured reactors.[3] The main challenge in reactor design is efficient heat management, which is essential due to the highly exothermic reaction.

In three phase $CO_2$ methanation (3PM), a slurry bubble column reactor is used, and a schematic of the reactor is shown in Fig. 1.

In the slurry bubble column reactor, catalyst particles are suspended in the liquid phase and fluidized by the gas flow entering from the bottom through a gas sparger. The incoming gas flow creates a high degree of mixing that allows isothermal operation of the reactor.[7] The reactor

[a] Engler-Bunte-Institut - Fuel Technology, Engler-Bunte-Ring 1, 76131 Karlsruhe, Germany. E-mail: mathias.held@kit.edu
[b] Institute of Catalysis Research and Technology, Hermann-von-Helmholtz-Platz 1, 76344 Eggenstein-Leopoldshafen, Germany

Open Access Article. Published on 10 December 2025. Downloaded on 2/1/2026 6:07:50 PM.
This article is licensed under a Creative Commons Attribution 3.0 Unported Licence.

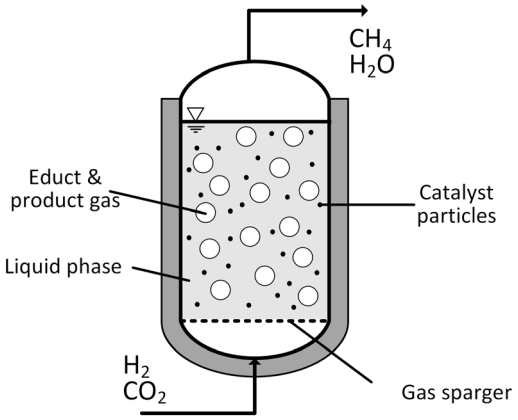


Fig. 1 Schematic drawing of a slurry bubble column reactor used for three phase $CO_2$ methanation.

demonstrates robustness under dynamic operation, with only a moderate temperature increase observed during a 100% change in gas load.[1]

Dibenzyl toluene is used as a liquid phase due to its high thermal stability, low vapor pressure, high gas solubility and favorable hydrodynamic properties.[8] Lefebvre[9] determined the reaction kinetics of three phase $CO_2$ methanation as a function of gas concentrations in the liquid phase.

**Catalyst deactivation in three phase $CO_2$ methanation.** At elevated temperatures, DBT is prone to decomposition[10–12] primarily forming benzyl toluene, benzene, toluene, xylene and methane.

DBT decomposition leads to catalyst deactivation due to carbon deposition.[13] Catalyst deactivation occurs at temperatures above $T_R > 260$ °C resulting in a reduction of the $CO_2$ methanation reaction rate by approximately 50%.

### 2.2 DBT hydrogenation in three phase methanation

Dibenzyl toluene is also discussed as a liquid organic hydrogen carrier (LOHC) in the literature.[14,15] Each DBT molecule can bind up to 9 $H_2$ molecules as shown in reaction eqn (2).

$$C_{21}H_{20} + 9{\cdot}H_2 \rightleftharpoons C_{21}H_{38} \quad \Delta H_R = -588 \text{ kJ mol}^{-1} \tag{2}$$

The nickel catalyst used in 3PM is also active for DBT hydrogenation, and thus DBT hydrogenation is observed as a side reaction in three phase methanation.[16]

To describe the hydrogenation reaction of DBT and determine the reaction rate $r_{DBT}$, the degree of hydrogenation DoH is used. It quantifies the fraction of hydrogenated double bonds in DBT, as defined in eqn (3). In three phase $CO_2$ methanation experiments, Marlotherm SH is used as the liquid phase, which is an isomeric mixture of DBT molecules with a DoH of 0. As hydrogenation proceeds during methanation, an increase in DoH is observed over time.

$$\text{DoH} = \frac{N_{\text{hydrogenated double bonds}}}{N_{\text{initial double bonds}}} \tag{3}$$

All experiments in this work are conducted in a continuous stirred-tank reactor (CSTR). In this setup, DBT hydrogenation is operated in semi-batch mode; the $CO_2$ methanation reaction rate $r_{CO_2}$ increases until chemical equilibrium of DBT hydrogenation is reached.

In DBT hydrogenation experiments, deactivation of the Ni catalyst was also observed. The hydrogenation reaction rate $r_{DBT}$ decreases with increasing reactor temperature.[13] This behavior is attributed to the $CO_2$ methanation reaction and catalyst deactivation at reactor temperatures above $T_R > 260$ °C.

### 2.3 Determination of reaction kinetics in three phase systems

Continuous stirred-tank reactors can be used to determine reaction kinetics in three phase systems. The concentration profile of reactants in the CSTR is illustrated in Fig. 2.

In a CSTR, ideal mixing is assumed in both the gas and the liquid phases, so a concentration gradient is only present at the gas–liquid interface. The solubility of the educt and product gases in the liquid phase is described by the Henry coefficient $H_{i,px}$, as defined in eqn (4):

$$H_{i,px} = \lim_{x_i \to 0} \frac{p_i}{x_i} \tag{4}$$

The Henry coefficient $H_{i,px}$ represents the ratio between the gas partial pressure $p_i$ and the concentration of the component in the liquid phase $x_i$.

A second concentration gradient arises from the reaction occurring on the catalyst surface: it is typically assumed that the entire catalyst surface is wetted by the liquid phase, so the reaction takes place within the liquid phase on the catalyst surface, and is described by the reaction rate $r_{i,liq}$ (2).

There are two main approaches to determine the reaction kinetics for three phase systems in a CSTR:

- Using the partial pressures of reactants in the gas phase to derive reaction kinetics.
- Using the concentrations of reactants in the liquid phase to derive reaction kinetics.

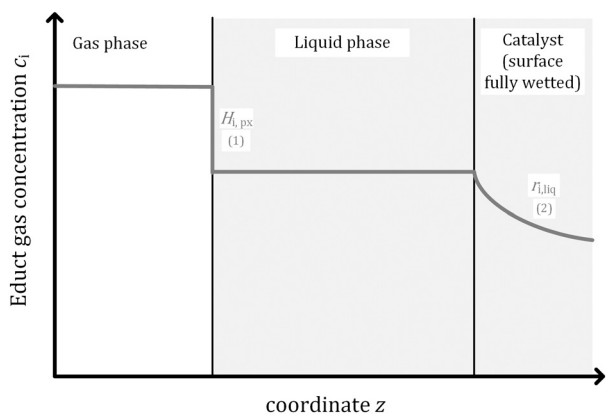


Fig. 2 Concentration profile of an educt gas species in an ideally mixed CSTR for a fully wetted catalyst particle.

Open Access Article. Published on 10 December 2025. Downloaded on 2/1/2026 6:07:50 PM.
This article is licensed under a Creative Commons Attribution 3.0 Unported Licence.

Both approaches are discussed in the literature for three phase syntheses, such as slurry-phase Fischer–Tropsch synthesis.[17] In the first approach, the reaction rate equation is derived using the gas-phase partial pressure $p_i$ of the reactants.[18–20] As a result, the reaction rates obtained not only describe the reaction at the catalyst surface $r_{i,liq}$ (2) but also incorporate gas solubility *via* the Henry coefficient $H_{i,px}$ (1). An advantage of this method is that Henry coefficients do not need to be determined for the used system.

However, a limitation is that the resulting reaction kinetics is only valid for the specific liquid phase and hydrodynamic conditions investigated, and cannot be applied to reactor designs where additional mass transport resistances are present.

In the second approach, reaction kinetics is derived based on liquid phase concentrations of the reactants.[21–24] This requires determining the Henry coefficients of the reactants for the specific liquid phase and reaction conditions. The concentration of reactants in the liquid phase can then be calculated from their gas-phase partial pressures using the Henry coefficient. An advantage of this approach is that the resulting reaction kinetics are applicable to reactor designs where mass transport limitations are present.

In the slurry bubble column reactor used for $CO_2$ methanation, mass transport of educt gases from gas bubbles to the catalyst surface must be considered. Lefebvre demonstrated that mass transfer from the gas/liquid interphase to the liquid bulk, described by the volumetric liquid-side mass-transfer coefficient $k_L a_i$, along with the chemical reaction, is the relevant step in determining the effective reaction rate.[25] Therefore, $k_L a_i$ must be considered in reactor design, which is not accounted for in the CSTR (see Fig. 2). This is only feasible if reaction kinetics based on liquid phase concentrations are available.

Lefebvre determined the reaction kinetics of three phase $CO_2$ methanation based on liquid phase concentrations.[9] To calculate the concentration of reactants in the liquid phase, the Henry coefficients of the educts $CO_2$ and $H_2$ as well as the products $CH_4$ and $H_2O$ were measured over the relevant temperature range.[25] Using these coefficients, the concentration of educt and product gases in the liquid phase $c_{i,DBT}$ can be calculated from their gas-phase partial pressures $p_i$ (see eqn (4)). A reaction rate equation was derived from 91 $CO_2$ methanation experiments conducted in a CSTR:[9]

$$r_{CO_2} = 3.90699 \times 10^5 \cdot \exp\left(-\frac{79\,061}{R \cdot T}\right) \cdot \frac{c_{H_2,L}^{0.3} \cdot c_{CO_2,L}^{0.1}}{\left(1 + c_{H_2O,L}\right)^{0.1}} \cdot K \quad (5)$$

Here, $K$ represents the limitation of the reaction rate due to chemical equilibrium and is calculated as a function of the gas-phase partial pressures $p_i$:

$$K = 1 - \frac{{p_{H_2O}}^2 \cdot p_{CH_4}}{{p_{H_2}}^4 \cdot p_{CO_2}} \cdot \frac{{p_0}^2}{K_{eq}} \quad (6)$$

# 3 Materials & methods

In the following chapters, experiments involving two distinct reactions will be presented: DBT hydrogenation and three phase $CO_2$ methanation. In both experiments, the same catalyst and liquid phase are used. In DBT hydrogenation, only $H_2$ is introduced into the reactor, whereas in $CO_2$ methanation, both $H_2$ and $CO_2$ are supplied.

## 3.1 Experimental setup

All experiments are conducted in a continuous stirred-tank reactor (CSTR). The absence of mass transfer limitations was validated by varying the stirrer speed. Gas solubilities, described by Henry coefficients,[25] are used to determine reaction kinetics based on reactant concentrations in the liquid phase.

For all experiments, a commercially available $Ni/SiO_2$ catalyst and Marlotherm SH as the liquid phase are used. The catalyst is reduced in a fixed-bed reactor at $T_R$ = 430 °C for $t_{red}$ = 72 h according to the manufacturer's instructions and then transferred to the liquid phase in the CSTR under an inert atmosphere to prevent oxidation. The flow rate of educt gases $\dot{n}_i$ is controlled using mass flow controllers. Electrical heating is used to set the reactor temperature $T_R$, and a pressure regulator controls the reactor pressure $p_R$. To determine the $CO_2$ methanation reaction rate $r_{CO_2}$, the product gas composition is analyzed using an Agilent 490 Micro GC. During the experiment, liquid phase samples are taken to determine the Degree of Hydrogenation (DoH) of the liquid phase and calculate the DBT hydrogenation reaction rate $r_{DBT}$. The loss of liquid phase and catalyst due to sampling from the CSTR is accounted for in the calculation of reaction rates.[16]

## 3.2 Determination of reaction rates

To determine the reaction kinetics of $CO_2$ methanation, experimental reaction rates are calculated from the product gas composition. Reaction rates for DBT hydrogenation are determined by sampling the liquid phase and measuring the DoH.

**3.2.1 Determination of the $CO_2$ methanation reaction rate.** The mole fraction of $CO_2$ in the product gas is measured *via* gas analysis. Using the molar flow rate of $CO_2$ in the educt gas, the $CO_2$ conversion is calculated according to eqn (7):

$$X_{CO_2}(t) = \frac{\dot{n}_{CO_2,in}(t) - \dot{n}_{CO_2,out}(t)}{\dot{n}_{CO_2,in}(t)} \quad (7)$$

To calculate the $CO_2$ methanation reaction rate from $X_{CO_2}$, both the molar flow rate of $CO_2$ and the mass of the catalyst must be considered. This ratio is expressed by the modified residence time of $CO_2$ $\tau_{mod,CO_2}$:

$$\tau_{mod,CO_2} = \frac{m_{cat}}{\dot{n}_{CO_2,in}} \quad (8)$$

Using $X_{CO_2}$ and $\tau_{mod,CO_2}$, the $CO_2$ methanation reaction rate $r_{CO_2}$ is calculated as:

Open Access Article. Published on 10 December 2025. Downloaded on 2/1/2026 6:07:50 PM.
This article is licensed under a Creative Commons Attribution 3.0 Unported Licence.

$$r_{CO_2} = \frac{X_{CO_2}}{\tau_{mod,CO_2}} \quad (9)$$

**3.2.2 Determination of the DBT hydrogenation reaction rate.** The reaction rate of DBT hydrogenation is determined by sampling the liquid phase. The DoH of each sample is calculated from density measurements using the following correlation:[13]

$$\mathrm{DoH} = 22.45 - 37.36\cdot\left(\frac{\rho_{DBT}}{\mathrm{g\ cm^{-3}}}\right) + 15.19\cdot\left(\frac{\rho_{DBT}}{\mathrm{g\ cm^{-3}}}\right)^2 \quad (10)$$

The density of the liquid phase samples is measured using an Anton Paar 4200 M benchtop vibration tube density meter. Samples are taken throughout the experiment to observe the change in DoH over Time on Stream (ToS). The DBT hydrogenation reaction rate $r_{DBT}$ is calculated as:

$$r_{DBT} = \frac{n_{DBT}}{m_{cat}}\cdot\frac{[\mathrm{DoH}(t) - \mathrm{DoH}(t_0)]}{[t - t_0]} \quad (11)$$

The change in DoH is evaluated for values below DoH $< 0.2$ to minimize the influence of chemical equilibrium. Similar to the $CO_2$ methanation reaction rate (eqn (9)), both the molar amount of DBT $n_{DBT}$ and the catalyst mass $m_{cat}$ are considered.

### 3.3 Evaluation of catalyst deactivation

In three phase $CO_2$ methanation, catalyst deactivation due to carbon deposition is observed.[13] The impact of catalyst deactivation on both $CO_2$ methanation and DBT hydrogenation is also addressed in this work. The detailed experimental procedure for determining the loss in catalytic activity is described in the previous work.[13]

Catalyst activity is calculated as the ratio of the measured reaction rate $r_i$ to the reaction rate without deactivation $r_{i,0}$. This approach is applied to both reactions:

$$a_i = \frac{r_i}{r_{i,0}}; \quad i = CO_2, \mathrm{DBT} \quad (12)$$

## 4 Results

In this chapter, the wetting behavior of the catalyst particle with the liquid phase DBT is discussed for three phase systems, and a partial wetting theory is introduced. This theory is validated by analyzing the influence of catalyst deactivation on $CO_2$ methanation and DBT hydrogenation activity. Furthermore, reaction kinetics under steady state conditions for the deactivated Ni catalyst is determined.

### 4.1 Catalyst wetting in three phase reactions

DBT hydrogenation involves DBT as a liquid phase reactant, and therefore only occurs at active sites on the catalyst surface that are wetted by DBT. In contrast, the $CO_2$ methanation reaction occurs both at sites covered by the liquid phase and at those directly exposed to the gas phase. Lefebvre[9] assumed that the entire catalyst surface is wetted by DBT and derived the reaction kinetics based on liquid phase concentrations. However, analysis of the used catalyst used shows that the pore sizes range from $d_p$ = 0.5 to 300 nm, making partial wetting of the catalyst pores more likely. Diffusion limitations for DBT molecules in catalyst pores have been shown to occur for pore sizes below $d_p < 30$ nm.[26,27]

A schematic illustration of a partially wetted catalyst is shown in Fig. 3. The gaseous reactants dissolve in the liquid phase and react at the catalyst surface. Active sites wetted by DBT are involved in both $CO_2$ methanation (blue sites) and DBT hydrogenation (orange sites). In small pores, where DBT does not wet the gas–solid interface, only $CO_2$ methanation occurs.

Since catalyst deactivation is caused by DBT decomposition and carbon deposition on the catalyst surface, only the DBT-covered surface areas, *i.e.* the larger pores, are affected. This consideration is discussed in detail in the following chapter to validate the partial wetting theory. Due to partial wetting of the catalyst, reaction kinetics based on liquid-phase concentrations are not intrinsic. They include the reaction at liquid-covered active sites as well as Henry coefficients, mass transport and reaction at active sites within gas-filled catalyst pores.

In Fig. 4, the concentration profile of an educt gas species in a CSTR with a partially wetted catalyst pore is illustrated. Due to ideal mixing in the CSTR, the concentration remains constant in both the gas and liquid bulk phases. The Henry coefficient describes the solubility of reactants in the liquid phase. The catalyst pores are only partially wetted by DBT, and the educt gas concentration decreases along the pore length due to the reaction at active sites covered by the liquid phase. In this region, no diffusion limitation of the gas species is observed.[25] At the gas–liquid interface inside the catalyst pores, Henry coefficients can be used to calculate the gas-phase partial pressure. In the gas-filled pores, both mass

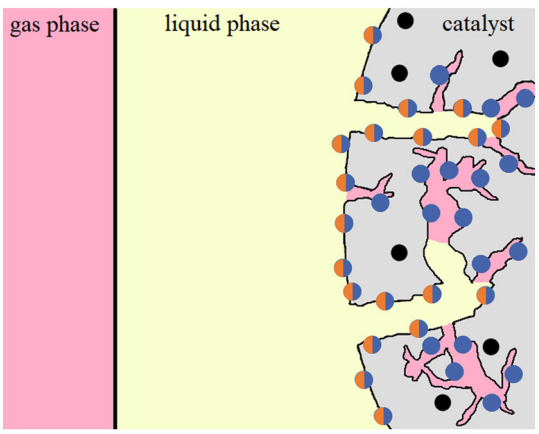


Fig. 3 Schematic drawing of partial wetting of the Ni catalyst by DBT with active sites for DBT hydrogenation (orange) & $CO_2$ methanation (blue).

Open Access Article. Published on 10 December 2025. Downloaded on 2/1/2026 6:07:50 PM.
This article is licensed under a Creative Commons Attribution 3.0 Unported Licence.

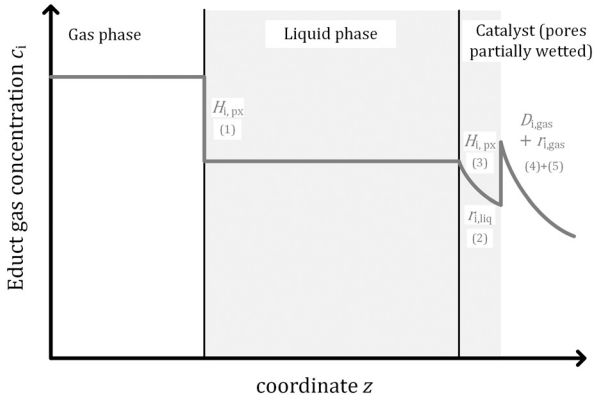


Fig. 4 Concentration profile of an educt gas species in a CSTR for a partially wetted catalyst pore.

transport resistances and chemical reaction must be considered to describe the educt gas concentration profile.

### 4.2 Validation of the partial catalyst wetting theory

To validate the partial wetting theory for the catalyst used in three phase $CO_2$ methanation, catalyst deactivation was evaluated in detail for both $CO_2$ methanation and DBT hydrogenation. When catalyst deactivation was observed in $CO_2$ methanation, the maximum loss in catalytic activity was consistent across all experiments, regardless of reactor temperature or pressure. After deactivation, the catalytic activity was $a_{CO_2} \approx 50\%$.[13] This observation can be explained by partial wetting of the catalyst surface: deactivation is caused by DBT decomposition and carbon deposition, which occur only on the surface areas covered by DBT. Therefore, deactivation is limited to the fraction of catalyst surface wetted by DBT. Even when the wetted surface is fully deactivated, $CO_2$ methanation still proceeds in the gas-filled catalyst pores. In contrast, if the entire catalyst surface was covered by DBT, complete deactivation would be expected, and no catalytic activity would be observed after sufficient Time on Stream.

In Fig. 5, the DoH is shown for two different $CO_2$ methanation experiments. The reaction conditions were identical in both cases: one experiment used a fresh Ni catalyst, while the other used a deactivated catalyst. To induce deactivation, the reactor temperature was set to $T_R$ = 320 °C for ToS = 120 hours. As a result, a DoH of approx. 10% was already present at the start of the experiment.

Since DBT hydrogenation occurs as a side reaction in three phase $CO_2$ methanation, the DoH increases over ToS in both experiments. However, for the deactivated catalyst, the increase in DoH is significantly less pronounced compared to the fresh catalyst. To evaluate catalytic activity for DBT hydrogenation, the reaction rates $r_{DBT}$ were compared. These rates were calculated using the slope of the DoH curves (see eqn (11)). For the deactivated catalyst, an activity of only $a_{DBT}$ = 10% was observed. This result demonstrates that DBT hydrogenation is more strongly affected by catalyst deactivation than $CO_2$ methanation ($a_{CO_2} \approx 50\%$). This can be attributed to the partial wetting of the catalyst surface: DBT hydrogenation occurs exclusively on DBT-covered active sites, which are also the sites affected by deactivation. In contrast, $CO_2$ methanation is less impacted, as it also takes place in the gas-filled pores, which remain active.

In Fig. 6, the catalytic activity for $CO_2$ methanation $a_{CO_2}$ is shown over Time on Stream for two different experiments. The reaction conditions were identical, with the reactor temperature of $T_R$ = 320 °C chosen to induce catalyst deactivation. In these experiments, two catalysts with distinct mean pore diameters – $d_p$ = 30 nm and $d_p$ = 45 nm, respectively – were compared. Details of the catalyst synthesis procedure are provided in the SI. The catalysts were characterized by $N_2$ physisorption; the corresponding adsorption–desorption isotherms and pore size distributions are presented in Fig. S1, while their textural and structural properties are summarized in Table S1. The nickel loading,

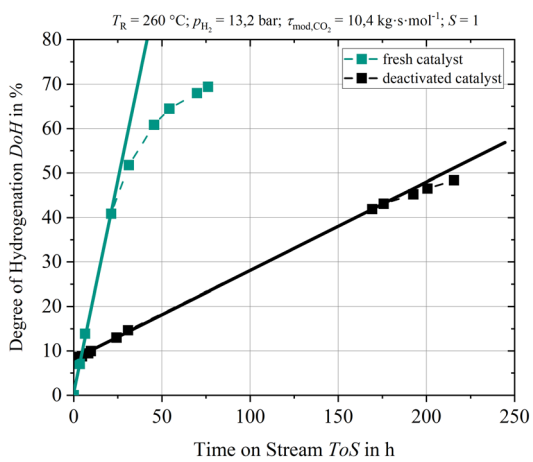


Fig. 5 Evolution of Degree of Hydrogenation over Time on Stream for two $CO_2$ methanation experiments with the same reaction conditions for fresh and deactivated catalysts.

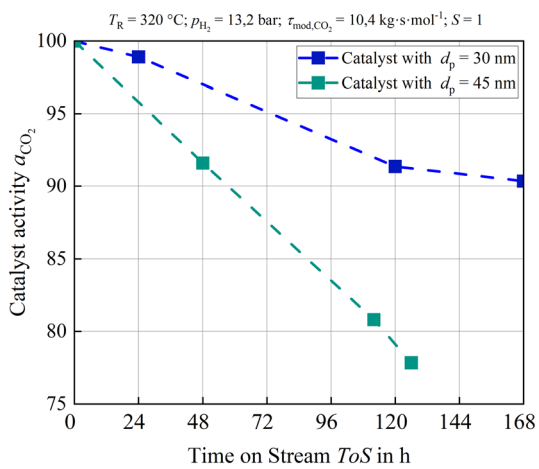


Fig. 6 Catalyst activity for $CO_2$ methanation over Time on Stream at $T_R$ = 320 °C. Comparison of two catalysts with different mean pore diameters $d_p$.

Open Access Article. Published on 10 December 2025. Downloaded on 2/1/2026 6:07:50 PM.
This article is licensed under a Creative Commons Attribution 3.0 Unported Licence.

determined by ICP-OES, is reported in Table S2. XRD patterns of the catalysts are shown in Fig. S2.

In both cases, a loss of catalytic activity was observed. However, for the catalyst with larger pore diameter $d_p$, the loss in activity was greater compared to the catalyst with smaller $d_p$. Smaller pore diameters result in a lower fraction of the catalyst surface wetted by DBT, meaning less surface is susceptible to deactivation. Consequently, the loss in catalytic activity is reduced for catalysts with smaller pore diameters as fewer DBT-covered sites are affected.

### 4.3 Reaction kinetics for stationary operation of three phase $CO_2$ methanation

At temperatures above $T_R > 260$ °C, catalyst deactivation is observed in three phase $CO_2$ methanation. Under these conditions, the reaction kinetics developed by Lefebvre *et al.*[9] is no longer valid.

In Fig. 7, the experimental reaction rate of $CO_2$ methanation $r_{CO_2}$ is shown over Time on Stream at $T_R = 320$ °C. Additionally, the reaction rate predicted by Lefebvre's kinetics[9] is plotted for the same reaction conditions. At the chosen temperature, catalyst deactivation occurs, and $r_{CO_2,exp}$ decreases with ToS. At the beginning of the experiment, the kinetic model accurately describes the experimental reaction rate. However, after the first few hours a sharp decline in $r_{CO_2,exp}$ is observed, which can be attributed to the formation of a carbon layer on the DBT-covered catalyst surface. After ToS ≈ 6 h, the reaction rate continues to decrease, but at a slower rate, due to limited remaining surface area available for further carbon deposition. After ToS ≈ 120 h, steady state is reached, and $r_{CO_2,exp}$ significantly deviates from $r_{CO_2,kinetics}$. Thus, the reaction kinetics developed by Lefebvre *et al.*[9] are only applicable in the absence of catalyst deactivation, which corresponds to temperatures below $T_R \leq 260$ °C.

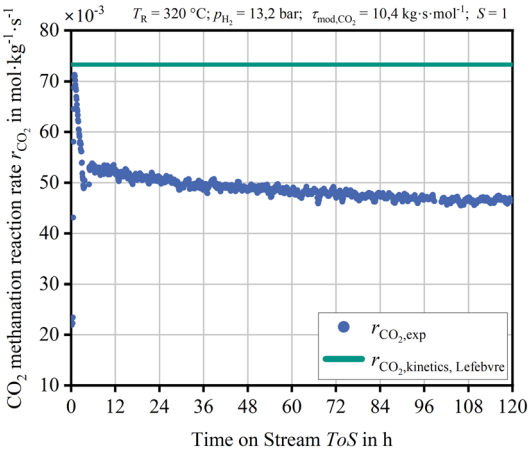


**Fig. 7** The $CO_2$ methanation reaction rate $r_{CO_2}$ over Time on Stream at $T_R = 320$ °C and the reaction rate calculated with reaction kinetics determined by Lefebvre *et al.*;[9] experimental data provided by Holfelder.[28]

For the application of three phase $CO_2$ methanation in slurry bubble column reactors, higher temperatures are generally preferred to achieve high $CO_2$ conversion. However, under these conditions deactivation occurs, and reaction kinetics suitable for steady state operation is required for reactor design. In this work, reaction kinetics for steady state operation considering catalyst deactivation have been determined for the typical reaction conditions in three phase $CO_2$ methanation. To achieve steady state operation, the catalyst was intentionally deactivated at $T_R = 320$ °C until a stable reaction rate was reached (see ToS ≈ 120 h in Fig. 7). Subsequently, reaction conditions were adjusted according to the ranges provided in Table 1.

After deactivation at $T_R = 320$ °C, steady state operation is achieved and the methanation reaction predominantly occurs in the gas-filled catalyst pores. Reaction kinetics was determined based on liquid phase concentration of the reactants, as mass transfer in the catalyst pores depends only on the catalyst properties and reaction conditions, not on the reactor configuration. Henry coefficients determined by Lefebvre[25] were used to calculate liquid phase concentrations from gas phase partial pressures.

In total, 72 data points were used to derive the kinetic rate equation for steady state operation of three phase $CO_2$ methanation:[29]

$$r_{CO_2} = 10^4 \cdot \exp\left(-\frac{66.93\ \text{kJ mol}^{-1}}{R \cdot T}\right) \cdot \frac{c_{H_2,L}^{0.63} \cdot c_{CO_2,L}^{0.07}}{\left(1 + c_{H_2O,L}\right)^{0.36}} \cdot K \quad (13)$$

Here, $K$ describes the limitation of $r_{CO_2}$ due to chemical equilibrium as defined in eqn (6).

## Conclusions

In three phase $CO_2$ methanation, three reactions occur simultaneously: $CO_2$ methanation, DBT hydrogenation and DBT decomposition, the latter leading to catalyst deactivation *via* carbon deposition. In the literature, complete wetting of the catalyst particle is typically assumed for three phase systems. However, in this work, partial wetting of the catalyst particles in three phase $CO_2$ methanation was experimentally validated: the catalyst pores are not fully filled with the liquid phase DBT. Instead, small catalyst pores remain gas-filled, and consequently no DBT hydrogenation or decomposition occurs in these regions.

The following experimental observations were used to validate the partial wetting theory:

**Table 1** Range of process parameters for the development of a reaction rate equation for stationary operation of three phase $CO_2$ methanation

| Process parameter | Range |
|---|---|
| $T_R$ | 220–320 °C |
| $p_{CO_2}$ | 1–3.3 bar |
| $\frac{\dot{n}_{H_2}}{\dot{n}_{CO_2}}$ | 4–8 |
| $\tau_{mod,CO_2}$ | 10.3–164.3 kg s mol$^{-1}$ |

Open Access Article. Published on 10 December 2025. Downloaded on 2/1/2026 6:07:50 PM.
This article is licensed under a Creative Commons Attribution 3.0 Unported Licence.

- The loss in catalytic activity for $CO_2$ methanation is limited and consistent across all experiments. This is due to partial wetting: once the DBT-covered surface is fully deactivated, steady state operation is reached.
- The loss in catalytic activity for $CO_2$ methanation is more pronounced for catalysts with larger mean pore diameters. Larger pores result in more surface area being wetted with DBT and thus, a greater susceptibility to deactivation.
- The loss in catalytic activity is greater for DBT hydrogenation than for $CO_2$ methanation. Only the DBT-wetted active sites are involved in DBT hydrogenation and decomposition, which leads to carbon deposition. Therefore, activity loss is more significant for DBT hydrogenation.

For $CO_2$ methanation in a slurry bubble column reactor, high reactor temperatures are favorable to achieve high $CO_2$ conversion rates. However, at these temperatures, catalyst deactivation occurs due to DBT decomposition and carbon deposition. A kinetic rate equation was developed for steady state operation of $CO_2$ methanation with a deactivated catalyst, which describes the state relevant for technical application.

For catalysts with smaller pore size diameters of the catalyst support, less deactivation was observed. Future investigations into the support structure of the Ni catalyst, as well as nickel loading and dispersion may help maximize catalytic activity in three phase $CO_2$ methanation. The partial wetting of the catalyst particles was experimentally validated, and this finding is also relevant for determining reaction kinetics in other three phase systems.

## Author contributions

M. Monning: methodology, conceptualization, investigation, data curation, writing – original draft, and writing – review & editing. A. Asadli: resources and writing – review & editing. S. Bajohr: writing – review & editing and funding acquisition. M. Wolf: conceptualization and writing – review & editing. T. Kolb: writing – review & editing and funding acquisition.

## Conflicts of interest

The authors declare that there are no conflicts of interest.

## Data availability

All data supporting the findings in this article have been included in the figures and main manuscript. Further inquiries can be directed to the corresponding author.

Supplementary information (SI): detailed description od catalyst synthesis procedure and characterisation. See DOI: https://doi.org/10.1039/d5re00337g.

## Acknowledgements

This project was financially supported by the Federal Ministry of Education and Research in the scope of the project InnoSyn.

## Notes and references

1 S. Sauerschell, S. Bajohr and T. Kolb, *Energy Fuels*, 2022, **36**, 7166–7176.
2 P. Sabatier, *C. R. Hebd. Seances Acad. Sci.*, 1902, **134**, 514–516.
3 S. Rönsch, J. Schneider, S. Matthischke, M. Schlüter, M. Götz, J. Lefebvre, P. Prabhakaran and S. Bajohr, *Fuel*, 2016, **166**, 276–296.
4 M. Götz, J. Lefebvre, F. Mörs, A. McDaniel Koch, F. Graf, S. Bajohr, R. Reimert and T. Kolb, *Renewable Energy*, 2016, **85**, 1371–1390.
5 J. Ashok, S. Pati, P. Hongmanorom, Z. Tianxi, C. Junmei and S. Kawi, *Catal. Today*, 2020, **356**, 471–489.
6 P. Frontera, A. Macario, M. Ferraro and P. Antonucci, *Catalysts*, 2017, **7**, 59.
7 M. Held, D. Schollenberger, S. Sauerschell, S. Bajohr and T. Kolb, *Chem. Ing. Tech.*, 2020, **166**, 276.
8 M. Götz, Methanisierung im Dreiphasen-Reaktor, *PhD thesis*, Karlsruher Institut für Technologie, 2014.
9 J. Lefebvre, S. Bajohr and T. Kolb, *Fuel*, 2019, **239**, 896–904.
10 P. Modisha, P. Gqogqa, R. Garidzirai, C. N. M. Ouma and D. Bessarabov, *Int. J. Hydrogen Energy*, 2019, **44**, 21926–21935.
11 P. Modisha, R. Garidzirai, H. Güneş, S. E. Bozbag, S. Rommel, E. Uzunlar, M. Aindow, C. Erkey and D. Bessarabov, *Catalysts*, 2022, **12**, 489.
12 M. Xu, R. Gao, C. Shi, Z.-F. Huang, X. Zhang, J.-J. Zou and L. Pan, *Chem. Eng. Sci.*, 2024, **287**, 119754.
13 M. Held, A. Holfelder, S. Bajohr and T. Kolb, *React. Chem. Eng.*, 2025, DOI: 10.1039/D5RE00152H.
14 K. Müller, K. Stark, V. N. Emel'yanenko, M. A. Varfolomeev, D. H. Zaitsau, E. Shoifet, C. Schick, S. P. Verevkin and W. Arlt, *Ind. Eng. Chem. Res.*, 2015, **54**, 7967–7976.
15 P. Preuster, C. Papp and P. Wasserscheid, *Acc. Chem. Res.*, 2017, **50**, 74–85.
16 M. Held, A. Rieck, S. Bajohr and T. Kolb, *Int. J. Hydrogen Energy*, 2025, **132**, 166–173.
17 G. P. van der Laan and A. Beenackers, *Catal. Rev.: Sci. Eng.*, 1999, **41**, 255–318.
18 B. Todic, T. Bhatelia, G. F. Froment, W. Ma, G. Jacobs, B. H. Davis and D. B. Bukur, *Ind. Eng. Chem. Res.*, 2013, **52**, 669–679.
19 H. Eilers, M. I. González and G. Schaub, *Catal. Today*, 2016, **275**, 164–171.
20 J. Chang, L. Bai, B. Teng, R. Zhang, J. Yang, Y. Xu, H. Xiang and Y. Li, *Chem. Eng. Sci.*, 2007, **62**, 4983–4991.
21 J. Anfray, M. Bremaud, P. Fongarland, A. Khodakov, S. Jallais and D. Schweich, *Chem. Eng. Sci.*, 2007, **62**, 5353–5356.
22 S. Ledakowicz, H. Nettelhoff, R. Kokuun and W. D. Deckwer, *Ind. Eng. Chem. Process Des. Dev.*, 1985, **24**, 1043–1049.
23 W. Zimmerman, D. Bukur and S. Ledakowicz, *Chem. Eng. Sci.*, 1992, **47**, 2707–2712.
24 G. Graaf, J. Winkelman, E. Stamhuis and A. Beenackers, *Tenth International Symposium on Chemical Reaction Engineering*, 1988, pp. 2161–2168.
25 J. Lefebvre, *Three-phase CO2 methanation: Methanation reaction kinetics and transient behavior of a slurry bubble column reactor/ Jonathan Lefebvre*, Verlag Dr. Hut, München, 1st edn, 2019.

26 F. Auer, D. Blaumeiser, T. Bauer, A. Bösmann, N. Szesni, J. Libuda and P. Wasserscheid, *Catal. Sci. Technol.*, 2019, **9**, 3537–3547.
27 D. Zakgeym, T. Engl, Y. Mahayni, K. Müller, M. Wolf and P. Wasserscheid, *Appl. Catal., A*, 2022, **639**, 118644.
28 A. M. Holfelder, *Master's thesis*, Karlsruhe Institute of Technology, 2024.
29 V. Zaghini Francesconi, *Master's thesis*, Karlsruhe Institute of Technology, 2022.

Open Access Article. Published on 10 December 2025. Downloaded on 2/1/2026 6:07:50 PM.
This article is licensed under a Creative Commons Attribution 3.0 Unported Licence.


This journal is © The Royal Society of Chemistry 2025